

CHEMICAL STRUCTURAL INVESTIGATION OF THE COTTON FIBER BASE AND ASSOCIATED SEED COAT: FOURIER-TRANSFORM INFRARED MAPPING AND HISTOCHEMISTRY**David S. Himmelsbach and Danny E. Akin****U.S. Department of Agriculture****Athens, GA****Juheha Kim and Ian R. Hardin****University of Georgia****Athens, GA****Abstract**

Fourier-transform mid-infrared mapping and histochemical staining were employed to reveal the location and relative importance of chemical components involved with the base of cotton fibers and their associated seed coat. These two complementary techniques were focused on the nature of the chemical components that hold cotton fibers at their bases to the seed coat and with other portions of the seed coat fragment that are often found as part of the trash component of ginned cotton. Infrared results reveal waxes or long-chain alcohols adjacent to the shank of cotton fiber bases in the outer epidermal tissue in all regions of the cotton seed; uronate anions in the outer epidermis and pigment layers surrounding the bases of the fibers and strongly present in upper palisade layer tissue of all seed regions; compounds containing carbonyl functionality, acids and bases, at the juncture of the upper palisade and colorless layers; and tannin or pretannin-type aromatic structures in the outer pigment layer and interior to the cells in epidermal layer of all seed coat regions; lignin-type aromatics in the "colorless" layer of all regions of the seed coat. The infrared results are complemented by staining with Oil Red O for waxes, Ruthenium Red for pectins, acid phloroglucinol for lignins and vanillin-HCl for tannins. The results provide a better understanding of the fiber-seed interactions that are important to the development of methods for improving the separation of cotton fiber from seed coats. In turn, that would help to avoid breaking fibers and pulling out seed coat fragments with the fibers during ginning.

Introduction

The primary purpose of the ginning of cotton is to separate the cotton fibers from the seed. However, fragments of this structure often remain attached to the cotton lint and become a major source of "trash" that can ultimately

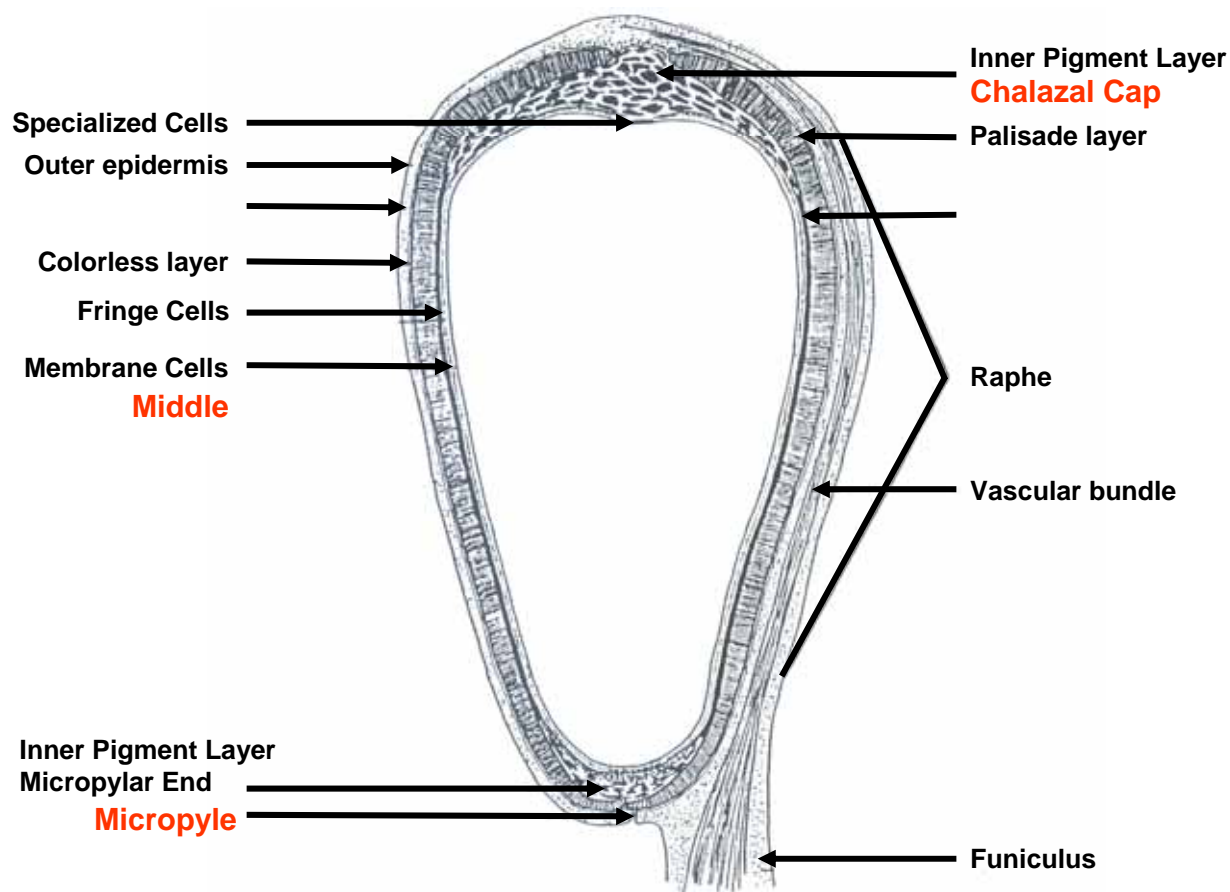


Figure 1. Diagram of the structure of the cottonseed. J. Leahy, "Structure of the Cottonseed", *Cottonseed and Cottonseed Products*, A. E. Bailey, Ed., Interscience, New York, 1948.

degrade the value of the cotton. The part of the seed that is typically broken off and remains with the lint is that from the chalazal end of the seed (see Figure 1). However, fibers are also attached to the middle and micropylar regions of the seed. The possibility exists that chemical structure of the seed differs in these regions. Studying the chemical structural differences among these regions could give some insight as to the reason for one region holding the fibers more rigidly than another.

Figure 2 is a schematic cross-sectional blow-up of the tissues involved with the attachment of fiber to the seed. Cotton fibers are produced from modified epidermal cells on the surface of the seed. The feet of the fiber are in contact with the outer pigment layer of the seed and the fiber shank surrounded by the cells of the outer epidermis. The strength of the attachment of the fibers to these tissues can influence the amount of short fiber produced and the amount of seed coat that remains attached after the cotton passes through the gin. The break point of the fiber from the seed is at or just above the outer surface epidermis, which is near the elbow (labeled as broken fiber in Figure 2).

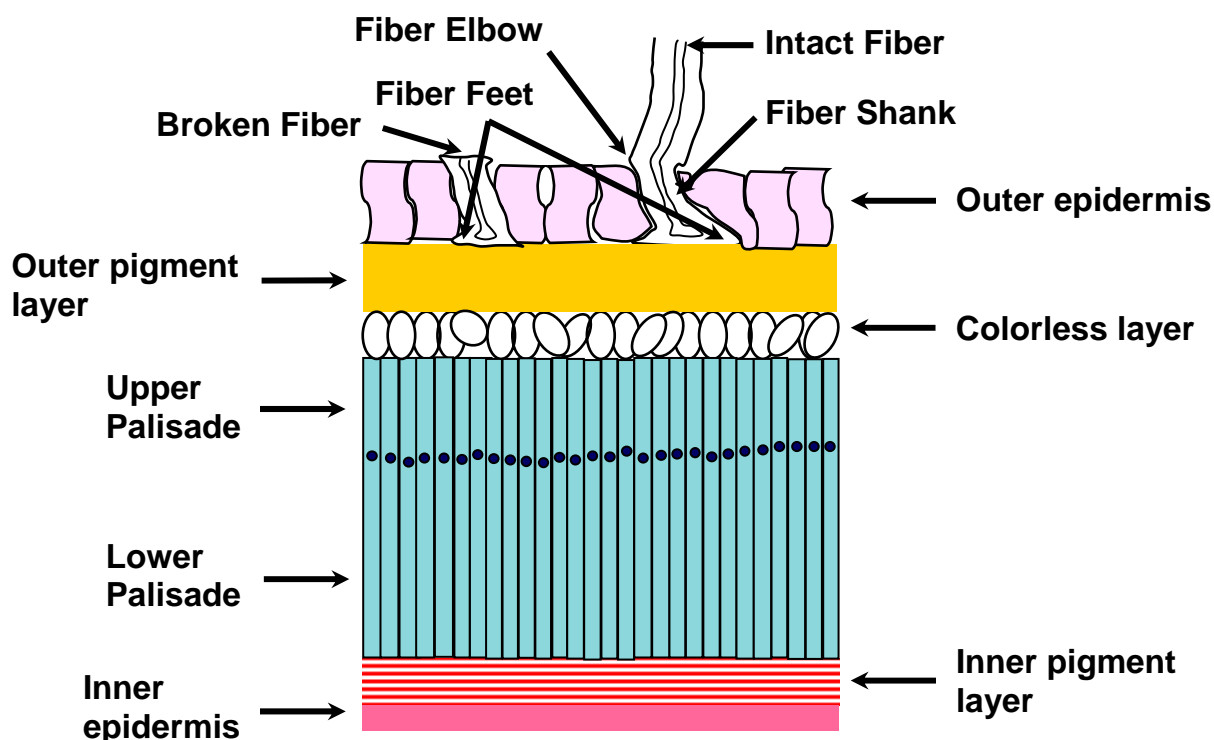


Figure 2. Schematic of cross-section of cotton seed coat showing anatomical components.

Electron microscopy has indicated that the primary wall at the elbow region has greater accumulations of electron dense cell wall material, implying a modified chemistry in this region (Virgil, 1996). Further electron microscopy studies with labeled antibodies indicated that cotton fibers had an outer layer of de-esterified pectin and extensin and an inner layer consisting of xyloglucans and cellulose (Vaughn, 1999). Since the primary wall has considerable amounts of non-cellulosic material (Wakelyn, 1998), studies suggest that other materials (i.e., sugars, proteins, waxes, aromatics) could contribute to the strength of the fiber-seed bond. Therefore, enzymes or reagents might be used that would disrupt components other than cellulose, thus preserving fiber strength as the fiber-seed bonds were weakened. Earlier work employed enzymes to reduce the fiber-seed bond (Wade, 1979), but, as pointed out by Vigil et al. (1979), the lack of enzyme purity may have caused some difficulty in interpreting these studies. Further, without adequate knowledge of chemical-structural relationships in cotton fiber and seed, the choice of appropriate enzymes to use is made more difficult.

Mid-infrared microspectroscopy can provide far-reaching results on chemical-structural relationships in biological materials (Stewart, 1996). Fourier-transform infrared (FT-IR) microspectroscopy has identified components within flax stems (Stewart, 1995). Himmelsbach et al., (1998a, 1998b & 1999) used both FT-IR and Raman microspectroscopy and microspectroscopic mapping to identify components within flax fiber bundles and associated tissues with relevance to enzyme-retting. In these studies, specific wavenumber absorbances permitted the locations of uronic components, waxes, and aromatics from prior work with reference materials. This methodology provides similar information on cotton fibers and fiber-seed interactions. The objective of this study was to employ FT-IR microspectroscopic mapping in parallel with staining reactions on various regions of cotton seeds to elucidate chemical-structural relationships, particularly in the fiber-seed coat regions.

Materials and Methods

Histochemical Staining

Embedding: Cotton seeds from Deltapine cotton were provided by Dr. O. Lloyd May from an experimental plot in Tifton, GA, and harvested in 2000 was used for this study. Five seeds were randomly selected and sectioned with a

razor blade in the chalazal, middle, and micropylar areas. Seed coat portions from each area were cut into 2 to 3 mm sections. The sections were dehydrated using a series of ethanol-water solutions with increasing concentrations of ethanol (50 %, 70 % and 100%). The ethanol in the sections was then replaced by infiltration solution. The infiltration solution (100 percent) was prepared by adding 1 gram of Catalyst (JB-4™ Embedding Kit, Polysciences, Inc.) to 100 ml of JB-4 Solution A™. Sections were immersed in a 50/50 infiltration-ethanol solution and then a 70/30 infiltration-ethanol solution for 1.5 hours each. Sections were then immersed in a 100 percent infiltration solution and kept overnight in a refrigerator. The sections were embedded in a freshly made embedding resin (15ml of fresh infiltration solution + 1ml Solution B™) and cured in a vacuum oven, which was purged with nitrogen gas until the resin hardened at room temperature.

Sectioning: The embedded sections were cut on a microtome using a dry glass knife instead of a knife with a water-boat because the JB-4™ is soluble in water. The sections were picked up by a syringe and collected on glass slides. The slides were heated lightly on a hot plate in order to adhere sections to the slide. Six μm was chosen as an ideal thickness since the sections were thin enough to be transparent and thick enough to get a good staining intensity.

Staining: Thin sections were stained with dyes to determine the location and identity of chemical constituents. The stains chosen and their substrates are as follows: Oil Red O for waxes (Achwal, 1985); Ruthenium Red for pectin (Jensen, 1962); acid phloroglucinol for lignin containing, α,β -unsaturated aromatic aldehydes (Clifford, 1975 and Jensen, 1962); and vanillin-HCl for tannins (Gardner, 1975). The samples were washed with distilled water after staining, and mounted in glycerin.

Light Microscopy: Stained and mounted sections were observed under bright-field microscopy. Stain intensity (0 = no color to 5 = intense color) was scored for specific tissues within the chalazal, middle, and micropylar regions of 5 seeds. Light microscopy images were also digitally captured for further comparison of results.

FT-IR

Sectioning: Additional seeds, randomly selected from the same lot as for histochemical staining, were free-hand cut in half with a razor blade. The seed halves were then frozen in doubly deionized water at -12°C onto object disks in a cryostatic microtome and subsequently cut into thin cross-sections, 6-8 μm thick, using disposable razor blade microtome knives. The cross-sections were transferred directly from the microtome knives to individual circular BaF₂ disks (13x2 mm). Sections were obtained from chalazal, middle, and micropylar regions and kept hydrated by maintaining the disks on water saturated paper towels in Petri dishes until usage. Just before mapping, the samples and disks were dried under an infrared lamp followed by equilibration (under desiccation over calcium sulfate) to room temperature. The sample disks were then mounted in Spectra-Tech (Thermo Spectra-Tech, Shelton, CT) compression cells and secured in the infrared microscope stage holder.

Mapping: FT-IR mapping was conducted using a Continuum™ microscope integrated with a Nicolet Magna 850 FT-IR bench (Thermo Nicolet, Madison, WI). The system utilized a globar source and a KBr beamsplitter, housed in the bench, and employed a liquid nitrogen cooled MCT/A (narrow band) detector, located in the microscope. The microscope was further equipped with an automated XYZ motorized stage that was operated in the autofocus (z-direction) mode under software control. Data collection, stage control and image data processing were performed using OMNIC E.S.P.™ ver. 5.2 (Thermo Nicolet, Madison, WI) in conjunction with Atlas™ (Thermo Spectra-Tech, Shelton, CT) software. Both visible images and infrared maps were obtained in the transmission mode, focused on the sample through an infinity corrected 32X Reflachromat™ (Schwartzchild type) objective and condenser. Visible images, obtained using a 3-CCD RGB camera (Panasonic GP-US522, Japan) attached by way of a trinocular to the microscope and also connected to the microcomputer through a video frame grabber, were digitally linked to the infrared maps.

Each pixel was collected so as to contain an infrared spectrum over the range of $4000\text{-}750\text{ cm}^{-1}$ at a spectral resolution of 8 cm^{-1} with 256 scans, a mirror physical velocity of 1.27 cm/sec and a bench aperture setting of 100 (10 mm) at a gain of 8. IR radiation was apertured in the microscope by double passing (redundantly aperturing) through a 20 μm square mask. Each pixel was a result of stepping, in 10 μm increments (over-sampling the apertured area), in both the X and Y directions. The total data collection time varied from 4-7 hr, depending on the

size of the region mapped. The bench was continuously purged with dry, CO₂ free, air and the microscope with zero grade N₂ during data acquisition. The spectral data were collected as interferograms that were apodized with a Happ-Genzel function prior to Fourier transformation to the frequency domain spectrum. Spectral data from the samples was ratioed against the background spectrum of a KBr crystal that had been placed within 100 μm of region of the sample that was imaged. The background was automatically updated after every 10th pixel. The resulting spectra were displayed in the absorbance mode. An automatic baseline adjustment was then applied to all of spectra to provide the final data matrix.

Profiles: Chemical profiles were produced from the mapping procedure by extracting and displaying specific absorptions on the basis of their band intensities from the entire map area to produce a profile for that band. These profiles produced sub-matrices of the data that were displayed in a 2-D pseudo-colored format. Five profiles were produced from the intensity of bands at: 2855, 1734, 1605/1640, 1514 and 1508 cm⁻¹ relative to local baselines at: 2881-2823, 1782-1686, 1693-1558 and 1558-1485 and 1543-1493 cm⁻¹ (respectively). The profiles for specific tissues of the chalazal, middle, and micropylar regions were scored in the same manner as with the histochemical staining results. Four profiles were also digitally captured for detailed comparison to the histochemical staining results.

Results

Histological staining scores

The scored histological results from staining of cross-sections with Oil Red O, Ruthenium Red, acid phloroglucinol and vanillin-HCl are given in Table I. Oil Red O positively stained only the surface of the fiber bases and the outer epidermis tissue in all three regions of the seed. In the case of Ruthenium Red, the outer and inner pigment layers, upper palisade and inner epidermis reacted strongly (4 or 5 score) with the stain regardless of whether the section was from the chalazal, middle or micropylar region. Acid phloroglucinol very weakly stained (0-1 score) the colorless layer, but no other tissues, in the chalazal region. It strongly to moderately stained the colorless layer and inner pigment layers in the middle region. In the micropylar region it stained the inner and outer pigment layers strongly and, to a lesser extent, the colorless layer. With vanillin-HCl, the strongest staining reaction appeared to occur inside of the cells of the outer epidermal layer and in inner and outer pigment layers of all seed regions. The colorless and lower palisade layers from the middle and micropylar regions were also stained significantly but to a lesser extent with this stain.

TABLE I. Scores on Staining Reactions of Seed Coat Sections ^a

Stain	Section Layer	Region of Seed Coat		
		<i>chalazal</i>	<i>middle</i>	<i>micropylar</i>
Oil Red O (wax stain)	fiber base ^b	5	5	5
	outer epidermis	5	5	5
	outer pigment	0	0	0
	colorless	0	0	0
	upper palisade	0	0	0
	lower palisade	0	0	0
	inner pigment	0	0	0
Ruthenium Red (pectin stain)	fiber base	1-2	1-2	1-2
	outer epidermis	2	1-2	0-1

	outer pigment	4	4-5	4-5
	colorless	0-1	0-1	0-1
	upper palisade	4	4	4-5
	lower palisade	1-2	0-1	1-2
	inner pigment	3-4	4	3-4
	inner epidermis	5	5	5
Acid Phloroglucinol				
(lignin-, unsat. aldehyde stain)	fiber base	0	0	0
	outer epidermis	0	0	0
	outer pigment	0	0	4-5
	colorless	0-1	5	2-3
	upper palisade	0	0	0
	lower palisade	0	0	0
	inner pigment	0	3-4	3-5
	inner epidermis	0	0	0
Vanillin-HCl				
(tannin stain)	fiber base	0	0	0
	outer epidermis ^c	0 (4)	0-1 (5)	0-1 (5)
	outer pigment	4	5	5
	colorless	0	3-4	3
	upper palisade	0	0-1	0
	lower palisade	2	3-4	2-3
	inner pigment	3	5	5
	inner epidermis	1-2	1-2	1
^a Numbers represent intensity from 0 [no reaction] to 5 [highest]				
^b Oil Red O stained only the surface of fiber base				
^c (Numbers in parenthesis) = inside the cells				

FT-IR profile scores

The score results from the mid-infrared profiles of the cross-sections from the three regions of the seed coat for the bands at 2855 cm⁻¹, 1605/1640 cm⁻¹, 1734 cm⁻¹ and 1514 cm⁻¹ are given in Table II. The profiles covered a reduced area of the cross-sections relative to those from the staining results due to a need to keep infrared data acquisition within a reasonable time limit (4-7 hr).

The 2855 cm⁻¹ band (for waxes) displayed the strongest absorbance in the outer epidermis tissue adjacent to or on the surface of the shank of the fiber base of the chalazal, middle and micropylar regions of the seeds. Weak absorbances were observed in the outer pigment layers of the middle and micropylar regions.

The 1734 cm⁻¹ band (for the carbonyl of acids or esters) and ratio of the 1605/1640 cm⁻¹ bands (for carboxylate anions/water) both displayed consistently strong absorbance (4-5 scores) in the upper palisade tissue of all regions of the seed coat. The 1734 cm⁻¹ band was the most intense on the border between the colorless and upper palisade layers. A shoulder at 1715 cm⁻¹ was prominent in the outer epidermal tissue that appeared to vary in a consistently with the 2855 cm⁻¹ band, suggesting they were related. Absorbance of the 1734 cm⁻¹ and 1605/1640 cm⁻¹ bands varied slightly within the other tissues but generally increased in the order middle < chalazal < micropylar and chalazal < micropylar < middle, respectively. The 1734 cm⁻¹ band showed more absorbance in the shank of the fiber base than with other parts of the fiber base.

TABLE II. Scores on Mid-Infrared Absorbance of Seed Coat Sections^a

Band	SectionLayer	Region of Seed Coat		
		<i>chalazal</i>	<i>middle</i>	<i>micropylar</i>
2855 cm ⁻¹ (waxes)	fiber base ^b	2-4	1-3	1-3

	outer epidermis ^b	2-5	2-5	3-5
	outer pigment	0	2-3	0-1
	colorless	0	1-2	0
	upper palisade	0	0	0
1734 cm ⁻¹ (carbonyl)	fiber base	0-3	0	0-1
	outer epidermis	0-3	0-1	1-4
	outer pigment	1-2	0-2	3-5
	colorless	2-3	2-3	2-3
	upper palisade	4-5	4-5	4-5
1605/1640 cm ⁻¹ (carboxylate anion)	fiber base	0-2	0-3	0-3
	outer epidermis	0-3	1-3	1-3
	outer pigment	1-3	3-4	2-5
	colorless	2-3	1-3	1-3
	upper palisade	4-5	4-5	4-5
1514 cm ⁻¹ (tannin-type aromatics)	fiber base	0-1	0	0
	outer epidermis	0-1	1	0-1
	outer pigment	0-2	1-3	2-5
	colorless	3-5	3-5	3-5
	upper palisade	0-4	0-3	0-4
1508 cm ⁻¹ (lignin-type aromatics)	fiber base	0-1	0	0
	outer epidermis	0-1	1	0-1
	outer pigment	0-2	1-3	2-5
	colorless	3-5	3-5	3-5
	upper palisade	0-4	0-3	0-4
^a Numbers based on 6 levels of intensity from 0 [below threshold] to 5 [at or above threshold]				
^b Surface of or adjacent to fiber base				

The fiber base shanks typically lacked any absorbance at 1605 cm⁻¹, as indicated by the ratioed result, but displayed absorbance in the area immediately adjacent to the fiber feet. The 1605 cm⁻¹ band indicated slightly more absorbance in the fiber feet of the micropylar region than in the chalazal and middle regions.

The 1514 cm⁻¹ band profile (for tannin-type aromatics) was at the higher frequency of the two aromatic bands. The 1514 cm⁻¹ band profile varied from no intensity to medium-high intensity at the upper palisade tissue showing greater intensity closer to the colorless layer. In the outer pigment, the 1514 cm⁻¹ band profile varied from medium to no intensity. The fiber feet displayed weak absorbance for this band. The outer epidermal tissues generally displayed weak to no absorbance intensity for the band at this frequency. In the colorless layer, the profile displayed the greatest intensity in the lower frequency band at 1508 cm⁻¹ (for lignin-type aromatics).

Detailed Comparison of Images in the Chalazal Region

The observation of the mid-infrared image profiles and the stained micrographs provide more detailed insights into the distribution of chemical components than can be expressed in generalized tables. Such a comparison is shown in Fig. 3. For reference, the visible CCD image of a 7 μm section of cotton seed coat from the chalazal end of a seed, obtained through the infrared microscope, is shown (Fig. 3a). In this image, two cotton fibers are evident that emerge from the outer epidermal layer and are attached to the underlying outer pigment layer of the seed coat. The fiber on the left clearly shows a well defined fiber foot whereas the one on the right is turned into the epidermal tissue at the "toes". The blue box delineates the region (120x90 μm) that was selected for infrared mapping. To the left of Figure 3a is shown an extracted spectrum from the ball of the foot of the fiber base on the left side of the sample showing the frequencies of the bands used for mapping pectate anions (1605 cm⁻¹) with water band

(1640 cm^{-1}) and that for tannin-type aromatics (1514 cm^{-1}). To the right of Figure 3a is shown an extracted spectrum from the colorless tissue of this sample showing the characteristic infrared bands for carbonyls (1734 cm^{-1}) and for lignin-type aromatics (1508 cm^{-1}).

Figure 3b is the infrared profile obtained based on the intensity (0.04-0.1 units) of the band at 2855 cm^{-1} , indicative of the anti-symmetrical C-H stretch vibration (Colthup, 1990). This band is primarily associated with waxes or long-chain alcohols. The color bar above this figure and for the subsequent infrared band profiles indicates, in pseudo-color, the relative intensity of absorbance of the band. All intensities below the lower threshold, on the left side of the bar, are given in white on the infrared maps and those above this value are displayed in increasingly greater increments, coded red through blue. Regions in blue are at or above the upper threshold value indicated on the right side of the bar. The high absorbance locations in Figure 2b are on the surface of or surround the upper part of the fiber base in the epidermal tissue. The location of the fiber feet in all of the infrared profiles are indicated by overlaid cartoons, since they are not readily observable except in a profile for cellulose (not shown).

Figure 3b may be compared to Figure 3f (below it) that shows the results of straining with Oil Red O. Oil Red O stain reacts in the same regions where medium to strong absorbance is indicated for the 2855 cm^{-1} infrared band. No determination as to the extent of the staining reaction can be made in the outer pigment layer due to the presence of opaque residual un-reacted stain adhered to this layer. The tissue layers show no absorbance at 2855 cm^{-1} . The infrared result confirms and provides the basis for the lack of actual reaction with the Oil Red O stain in these layers.

Figure 3c shows the infrared profile produced from the ratio of the intensity at 1605 cm^{-1} , which is the antisymmetric stretch for the carboxylate (COO^-) anion (Colthup, 1990), to that of bound water at 1640 cm^{-1} . With the over lapping of these to broad bands it was found best to use a ratio of band intensities to reduce the influence of water result rather than just using the single band for COO^- . The 1605 cm^{-1} band is most likely associated with salts of pectins but could be due to any galacturonate or glucuronate moiety, such as those associated with hemicelluloses. The band ratio yields numbers (0.7-1.7) that are not on the same scale as those of single band absorbance intensities, but do represent the band ratios. The COO^- profile produced fairly well agrees with the staining observed with Ruthenium Red (Fig. 3g). There is strong absorbance in the upper palisade tissue and sporadic low to medium absorbance within the outer epidermal and pigments tissues. The fiber feet appear to be surrounded by low to medium levels of uronate salts.

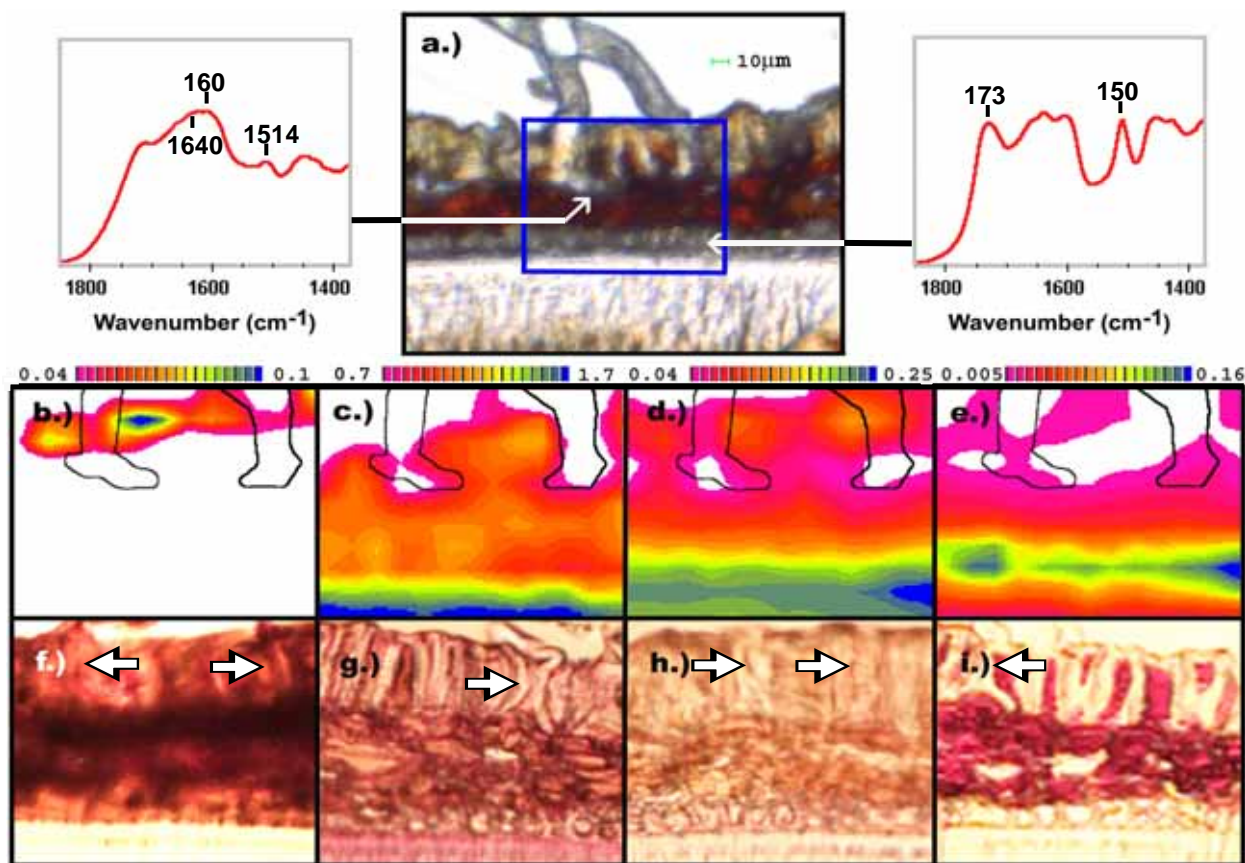


Figure 3. CCD visible image of 7 μm thick cross-section of seed coat from chalazal region showing two imbedded fibers (a.) with spectra extracted from points as indicated by arrows and showing relevant spectral bands. Infrared intensity maps from the region of blue box are shown for: waxes [2855 cm^{-1}] (b.), pectate anion [$1605/1640\text{ cm}^{-1}$] (c.), carbonyl [1734 cm^{-1}] (d.) and tannin-type aromatics [1514 cm^{-1}] (e.). Bars above maps indicate relative intensity the respective infrared bands. The locations of fiber bases in infrared maps are indicated by overlaid cartoons. Lower frames show comparative staining of similar seed coat sections with: Oil Red O (f.), Ruthenium Red (g.), acid phloroglucinol (h.) and vanillin-HCl (i.) with arrows indicating the location of fiber bases.

Figure 3d shows the infrared profile produced from the intensity of the 1734 cm^{-1} band, which is due to a carbonyl stretch (Colthup, 1990). This band is most likely associated with the uronic acids or their esters. Since the 1734 cm^{-1} band is strongly absorbed at the border of the upper palisade and colorless tissues and into the adjacent tissues and no absorbance for C-H stretch was observed near these tissues (Fig. 3b), the uronic carbohydrates of pectins or hemicelluloses are more likely present than waxes. There is medium to weak absorbance for the 1734 cm^{-1} band in the epidermal tissue, which contrary to the above, is likely associated with waxes, since C-H absorbance is observed in this tissue. Notably, there is only a weak indication of the uronic components in the pigment layer. Thus, the profile for the 1734 cm^{-1} band is also consistent with the results from the Ruthenium Red staining for pectins. Since phloroglucinol-HCl staining resulted (Fig. 3h) in only a faint reaction in the colorless tissue, it could not be corroborated very well with the infrared results. However, the aldehydic carbonyl that this stain reacts with could also have contributed to the 1734 cm^{-1} band.

Figure 3e shows the infrared profile for the 1514 cm^{-1} band due to aromatic ring breathing vibrations (Colthup, 1990). The strong band at 1508 cm^{-1} for lignin-type aromatics often overwhelms the 1514 cm^{-1} band and profiled by itself (not shown) is consistent with the histochemical results obtained with phloroglucinol-HCl (Fig. 3h) that shows only a light red coloration with this stain in the colorless layer. The band at 1514 cm^{-1} is more consistent with the histochemical results obtained with vanillin-HCl (Fig. 3i). The phloroglucinol-HCl stain does stain the

colorless layer in all regions, even though it only stains it very weakly in this tissue of the chalazal region (Fig. 3h). This result, when combined with the result from the C=O profile (Fig. 3d), suggests that the much of the aromatic species present in the colorless layer is lignin with an associated aldehyde moiety. The strong positive staining reaction with vanillin-HCl (Fig. 3i) in the epidermal and pigment layers exemplifies the sensitivity and specificity of this reaction for tannin type compounds. This reaction correlates with low levels of absorbance (0.005-0.16) selectively at 1514 cm^{-1} . The vanillin-HCl staining reaction required careful comparison to a 50% HCl control, as recommended by Gardner (Gardner, 1975), in these layers so that difference between the natural red color of the pigments (see Fig. 3a) and that produced by the stain could be discerned. The reaction was easier to discern, as a slightly lighter red color reaction, in the lower palisade tissue (not shown here), which very obviously indicated the presence of tannin type compounds there.

Discussion

While FT-IR has been used recently to identify chemical components in flax stems and (Himmelsbach, 1998 & 1999), to our knowledge no such work has been carried out on cotton-seed coat areas that involve fiber bases except for our recent work (Himmelsbach, 2003). In our previous work, we identified diagnostic infrared frequencies for particular compounds chosen as pure standards for materials present in plant tissues. In our recent work, the results of histochemical staining for particular compounds and IR mapping were compared, with the exception of the pectate anion, based on single discrete infrared band intensities bands as in previous work. The exception for the pectate anion is due to the proximity of the absorbance band for bound water at 1640 cm^{-1} to that for COO^- at 1605 cm^{-1} . By ratioing the 1605 cm^{-1} to the 1640 cm^{-1} band intensity the interference from the residual bound water on the 1605 cm^{-1} band is essentially eliminated and more reliable results are produced.

The relationship between the infrared results and the histochemical staining is especially evident in the comparison of sections of the chalazal region. The infrared absorbance observed for the 2855 cm^{-1} band on the on the shanks of the cotton fiber bases and in the outer epidermis tissue are the only locations that could be confirmed as staining with Oil Red O. Both of these methods are indicative of wax (Achwal, 1985 and Himmelsbach, 1998). In fact, no other tissues showed any actual reaction with this stain. These results indicate the presence of waxes or long-chain alcohols adjacent to the base of cotton fibers on the shank portion of their bases at their point of emergence from and elsewhere in the outer epidermis tissue that probably function to reduce the transfer of water across this barrier, thus limiting dehydration of the seed in drought conditions. The relatively strong staining reaction (score of 4) of the outer pigment layer tissues with Ruthenium Red, which generally stains for pectins but is not specific for this component (Jensen, 1962), was consistent with the observance of the absorbances at $1605/1640\text{ cm}^{-1}$ band for the carboxylate anion and at 1734 cm^{-1} of a further C=O containing material. This result is consistent with and would appear to confirm the presence of a mixture of carbohydrates with in this tissue layer. The infrared profiles additionally suggested that uronic-type carbohydrates existed adjacent to the colorless layer and surrounded the fiber feet. The latter observation suggests that pectate salts or other uronates may be important in anchoring fibers at their feet in the outer pigment tissue. Thus, treatment of this tissue to remove uronate-type components should aid in the release of fiber bases from the seed coat. Towards this end, the use of calcium chelators in conjunction with pectinolytic enzymes (Akin, 2000) or treatment with hemicellulases (Wakelyn, 1998) could facilitate the separation of fiber bases from the seed coat.

Finally, the results that the outer pigment layer and only the inside of the epidermal cells stained with vanillin-HCl and not at all with phloroglucinol-HCl in the chalazal region sections suggest that tannins or pre-tannins Colthup, 1990) are present in these tissues. Aromatic compounds with α , β -unsaturated aldehyde functional groups, which have been associated with lignin, are evidently lacking in this region. The fact that infrared absorption at 1514 cm^{-1} is observed at varying levels in the outer pigment layer and at the fiber feet is consistent with the results from the vanillin-HCl stain. Preliminary fluorescence results (Himmelsbach, unpublished) with excitation at 490 nm and emission above 530 nm suggested the weak and sporadic presence of anthocyanin or proanthocyanidin compounds in the outer pigment layer. Proanthocyanidins have been detected in the seed coats of other seeds (Beninger, 1999 and Todd, 1993). Thus, this result might be expected. Another result, previously obtained by treating the seed coat with laccase (Kim, 2000), indirectly supports the presence of tannins (proanthocyanidins) in this layer. Treatment with laccase made it more difficult to separate fiber bases from the seed coat. Tannins can be enzymatically induced

to form condensed structures and their presence could form complexes or rigid matrices that would make it difficult to remove fiber bases from the seed coat. Thus, not only the presence of pectins and hemicelluloses but tannins or a pre-tannin phenolic material must be considered in attempting to arrive at treatments to improve the release of fiber base from the seed coat.

Conclusions

To our knowledge, this is the first paper where FT-IR microspectroscopy has been used to discern chemical components with regions of cotton seed coats. While preliminary in nature, results establish the usefulness of the method and the close agreement with histochemical staining for important chemical constituents within all three regions of the seed. The presence of uronic moieties adjacent to the shank of the fiber base in the epidermal tissue and over the lower part of the foot of the fiber base suggests that an enzyme strategy could provide a means to weaken these associations and facilitate fiber release from the seed coat. The presence of tannin-type aromatic compounds in the pigment layers presents the possible necessity for dealing with the effect they may have on fiber removal from the seed coat, when polymerized. The fact that tissues in different regions of the seed -- chalazal, middle, and micropylar -- can be differentiated suggests that the specificity of the method could be exploited for analyzing changes in various cultivars and in plants grown under various environmental conditions.

Acknowledgments

Dr. O. Lloyd May of the Crop and Soil Sciences Department, The University of Georgia, Tifton, GA, is acknowledged for providing the seed cotton sample and Dr. Sadia Khalili of the Royal Institute of Technology, Stockholm, Sweden is acknowledged for diligence and expertise in sectioning the cotton seed coat tissue for infrared imaging.

References

- Akin, D. E., Dodd, R. B., Perkins, W., Henriksson, G., and Eriksson, K.-E. L., Spray Enzymatic Retting: A New Method for Processing Flax Fibers, *Textile Res. J.*, **2000**, 70, 486-494.
- Achwal, W. B., and Roy, N., A Rapid Staining Test to Assess Residual Wax in Pretreated Cotton Fabrics, *Colourage*, p. 11-14, May 16, **1985**.
- Bargeron, J. D., and Garner, T. H., Cottonseed Fragment Contamination and Fabric Imperfections, *Transactions of the ASAE*, **1991**, 34, 1575-1582 (1991).
- Beninger, C. W., and Hosfield, G. L., Flavonol Glycosides from Montcalm Dark Red Kidney Bean: Implications for the Genetics of Seed Coat Color in *Phaseolus vulgaris* L., *J. Agric. Food Chem.*, **1999**, 47, 4079-4082.
- Clifford, M. N., Specificity of Acidic Phloroglucinol Reagents, *J. Chromatogr.*, 1974, 94, 321-324.
- Colthup N.B., Daly L. H., "Introduction to Infrared and Raman Spectroscopy", 3rd Ed., Academic Press, Inc., San Diego, CA, **1990**.
- Freudenberg, K. and Weinges, K. Catechins and Flavonoid Tannins. In: "The Chemistry of Flavonoid Compounds", T. A. Geissman, Ed., The MacMillan Company, New York, **1962**, pp. 206-212.
- Fryxell, P. A., Morphology of the Base of Seed Hairs of Gossypium I. Gross Morphology, *Bot. Gazette*, **1963**, 124, 196-199.
- Gardner, R. O., Vanillin-Hydrochloric Acid as a Histochemical Test for Tannin, *Stain Tech.*, **1975**, 50, 315-317.
- Goynes, W. R., Ingber, B. F., and Triplett, B. A., Cotton Fiber Secondary Wall Development - Time Versus

Thickness, *Textile Res. J.*, 1995, 65, 400-408.

Himmelsbach, D. S., and Akin, D. E., Near-Infrared Fourier-Transform Raman Spectroscopy of Flax (*Linum Usitatissimum* L.) Stems, *J. Agric. Food Chem.*, **1998a**, 46, 991-998.

Himmelsbach, D. S., Khalili, S., and Akin, D. E., FT-IR Microspectroscopic Imaging of Flax (*Linum Usitatissimum* L.) Stems, *J. Cellular Mol. Biol.*, **1998b**, 44, 99-108.

Himmelsbach, D. S., Khalili, S., and Akin, D. E., Near-Infrared/Fourier-Transform Raman Microspectroscopic Imaging of Flax Stems, *Vib. Spectrosc.*, **1999**, 19, 361-367.

Himmelsbach, D. S., Akin, D. S., Kim, J., and Hardin, I. R. Chemical Structural Investigation of the Cotton Fiber Bae and Associated Seed Coat:Fourier-transform Infrared Mapping and Histochemistry. *Textile Res. J.*, **2003**, 73(4), 281-288.

Kim, J., Enhancement of Seed Coat Fragment Removal From Cotton by Enzymatic Treatment, Ph. D. Dissertation, University of Georgia, Athens, GA, **2000**.

Jensen, W. A., "Botanical Histochemistry," W. H. Freeman and Co., San Francisco, CA, **1962**.

Stewart, D., McDougall, G. J., and Baty, A. Fourier-Transform Infrared Microscopy of Anatomically Different Cells of Flax (*Linum usitatissimum*) Stems During Development. *J. Agric. Food Chem.*, **1995**, 43, 1853-1858.

Stewart, D., Fourier Transform Infrared Microspectroscopy of Plant Tissues, *Appl. Spectrosc.* **1996**, 50, 357-365.

Todd, J. J., and Vodkin, L. O., Pigmented Soybean (*Glycine max*) Seed Coats Accumulate Proanthocyanidins during Development. *Plant Physiol.*, **1993**, 102, 663-670.

Vaughn, K. C., and Turley, R. B., The Primary Walls of Cotton Fibers Contain an Ensheathing Pectin Layer, *Protoplasma*, 1999, **209**, 226-237.

Vigil, E. L., Anthony, W. S., Columbus, E., Erbe, E., and Wergin, W. P., Fine Structural Aspects of Cotton Fiber Attachment to the Seed Coat: Morphological Factors Affecting Saw Ginning of Lint Cotton, *Int. J. Plant Sci.*, **1996**, 157, 92-102.

Wade, C. P., and Rowland, S. P., The Cotton Fiber-Seed Bond: The Weakening Effects of enzymes and Wetting Agents, *Trans. ASAE*, Paper No. 79-1458, **1979**.

Wakelyn, P. J., Bertoniere, N. R., French, A. D., Zeronian, S. H., Nevell, T. P., Thibodeaux, D. P., Blanchard, E. J., Calamari, T. A., Triplett, B. A., Bragg, C. K., Welch, C. M., Timpa, J. D., Goynes, W. R. Jr., Franklin, W. E., Reinhardt, R. M., and Vigo, T. L., Cotton Fibers, in "Handbook of Fiber Chemistry" M. Lewin and E. M. Pearce, Eds., Marcel Decker, Inc., New York, **1998**, pp. 577-724.